GMJ 2024;35:228-235

DOI: http://dx.doi.org/10.12996/gmj.2023.3813

Comparison of Chest Computed Tomography Findings in Patients with H1N1 and Coronavirus Disease-2019 Pneumonia

H1N1 ve Koronavirüs Hastalığı-2019 Pnömonisi Olan Hastalarda Akciğer Bilgisayarlı Tomografi Bulgularının Karşılaştırılması

Sadullah Şimşek[1], Cihan Akgül Özmen[2]

[1]Department of Radiology, Nusaybin State Hospital, Mardin, Türkiye
[2]Department of Radiology, Dicle University Faculty of Medicine, Diyarbakır, Türkiye

ABSTRACT

Objective: In this study, we compared the differences between high-resolution computed tomography (CT) features of two types of viral pneumonia associated with H1N1 virus and coronavirus disease-2019 (COVID-19).

Methods: A total of 25 patients with H1N1 pneumonia were compared with 150 patients with COVID-19 pneumonia. The findings were analyzed by IBM SPSS Statistics for Windows, version 22 (IBM Corp., Armonk, N.Y., USA). CT findings were compared between groups by chi-square test, and scale variables were compared using the t-test. Finally, significant findings for the H1N1 or COVID-19 groups were evaluated by logistic regression analysis.

Results: The median age of COVID-19 pneumonia patients was 54.6±15.9 years, and the median age of H1N1 pneumonia patients was 46.2±12.4 years (p<0.01). H1N1 pneumonia patients were younger than COVID-19 pneumonia patients. Based on the distribution pattern, diffuse pattern, peripheral pattern, and bronchopulmonary infiltration were observed more frequently in COVID-19 pneumonia (46.0%, 80.7%, 49.3%, respectively, p<0.05). Mediastinal lymphadenopathy and pleural effusion were observed more frequently in patients with H1N1 pneumonia (24% and 36%, respectively, p<0.05). Logistic regression analysis demonstrated that advanced age and a diffuse-peripheral pattern indicated COVID-19 (p=0.031, p=0.029).

Conclusion: Most of the lesions caused by COVID-19 pneumonia are located in the peripheral region and near the pleura, whereas those caused by influenza virus pneumonia are far from the peripheral region.

Keywords: COVID-19, pneumonia, CT, influenza virus, coronavirus

ÖZ

Amaç: Bu çalışmada H1N1 virüsü ve koronavirüs hastalığı-2019 (COVID-19) ile ilişkili iki tip viral pnömoninin yüksek çözünürlüklü bilgisayarlı tomografi (BT) özellikleri arasındaki farkları karşılaştırmayı amaçladık.

Yöntemler: H1N1 pnömonisi olan toplam 25 hasta, COVID-19 pnömonisi olan 150 hasta ile karşılaştırıldı. Bulgular, IBM SPSS Statistics for Windows, sürüm 22 (IBM Corp., Armonk, N.Y., ABD) tarafından analiz edildi. BT bulguları gruplar arasında ki-kare testi ile ölçek değişkenleri ise t-testi kullanılarak karşılaştırıldı. Son olarak; H1N1 veya COVID-19 grupları için anlamlı olan bulgular lojistik regresyon analizi ile değerlendirildi.

Bulgular: COVID-19 pnömoni hastalarının medyan yaşı 54,6±15,9 ve H1N1 pnömoni hastalarının medyan yaşı 46,2±12,4 idi (p<0,01). H1N1 pnömoni hastaları, COVID-19 pnömoni hastalarından daha gençti. Dağılım paternine göre, COVID-19 pnömonisinde yaygın patern, periferik patern ve bronkopulmoner infiltrasyon daha sık görülür (sırasıyla, %46,0, %80,7, %49,3, p<0,05). H1N1 pnömonisinde mediastinal lenfadenopati ve plevral efüzyon daha sık gözlendi (sırasıyla, %24 ve %36; p<0,05). Lojistik regresyon analizi, ileri yaş ve yaygın periferik paternin COVID-19 ile anlamlı ilişkisini destekledi (p=0,031 ve p=0,029).

Sonuç: COVID-19 pnömonisinin neden olduğu lezyonların çoğu periferik bölgede ve plevraya yakın yerleşimlidir ve influenza virüsü pnömonisinin neden olduğu lezyonlar periferik bölgeden uzaktır.

Anahtar Sözcükler: COVID-19, pnömoni, BT, influenza virüs, koronavirüs

Address for Correspondence/Yazışma Adresi: Sadullah Şimşek, MD, Department of Radiology, Nusaybin State Hospital, Mardin, Türkiye
E-mail / E-posta: sadullahsimsek@gmail.com
ORCID ID: orcid.org/0000-0002-8322-7475

Received/Geliş Tarihi: 18.02.2023
Accepted/Kabul Tarihi: 02.06.2023

INTRODUCTION

A novel coronavirus known as coronavirus disease-2019 (COVID-19) was identified in lower respiratory tract samples from multiple patients in China, and this virus emerged during an epidemic caused by severe acute respiratory syndrome-coronavirus-2 (SARS-CoV-2) (1). The World Health Organization (WHO) classified this outbreak as an international public health emergency on January 30, 2020, and declared it a global pandemic on March 11, 2020 (2). Therefore, early detection, diagnosis, and isolation of COVID-19 patients are very important. The reverse transcriptase-polymerase chain reaction (RT-PCR) is the reference test used to confirm the diagnosis of COVID-19 infection. Recently, a large number of false-negative RT-PCR results have been reported (3). These results make diagnosis very difficult. Therefore, computed tomography (CT) of the chest is one of the best tools for primary diagnosis, estimation of disease severity, and monitoring of treatment. CT Manifestations are variable and may present as ground glass opacities (GGO), consolidation or combinations, crazy paving signs, interlobular septal thickening, air bronchogram, fibrous strictures, pleural effusions, and mediastinal lymphadenopathy. Most lesions are located in the peripheral subpleural region, mainly in the posterior or inferior lobe (4).

In spring 2009, several cases of human-to-human transmission by a subtype known as H1N1 were documented. By the end of May 2009, 41 countries had reported 11,000 cases and 85 deaths (5). Consequently, a level 6 pandemic was declared by the WHO. Clinical symptoms are mild in the majority of patients, with a flu-like illness (6). However, a small percentage of patients with H1N1 viral pneumonia may develop acute respiratory distress syndrome or severe cardiopulmonary failure. CT is an important tool for primary diagnosis, evaluation of complications that may develop after treatment, and determination of the degree of pulmonary disease (7). The radiologic findings reported were unilateral or bilateral GGO, either associated with focal or multifocal areas of consolidation or not. GGO and areas of consolidation have a predominantly bronchovascular and subpleural distribution, similar to organizing pneumonia (8,9). Recognition and analysis of these well-defined signs or patterns of involvement in chest CT are important because they can be treated at an early stage of the disease. In this study, we compared the differences between the high-resolution CT features of two types of viral pneumonia associated with H1N1 virus and COVID-19.

MATERIALS AND METHODS

The study was designed retrospectively. The study protocol was approved by the Mardin Provincial Health Directorate Scientific Study Board (approval number: E-37201737-949). Data search was performed to identify H1N1 and COVID-19 patients using the hospital's electronic archive system. For the identification of H1N1 virus infection, a specific period was set up from December 2010 to February 2013. Finally, 25 patients with PCR-confirmed H1N1 virus infection with chest CT were included in the study. In addition, the archive was scanned for patients with COVID-19 pneumonia between 1 July and 1 August 2020, and 150 patients were randomly selected COVID-19 patients with positive PCR results were included in the study. Patients with decompensated heart failure and lung malignancy were excluded from the study. Chest CT scans were obtained and re-evaluated using the hospital's Picture Archiving and Communication Systems.

CT images were obtained using 64-multidetector computed tomography (MDCT) scanners Brilliance Circular Edition (Philips) and 256-MDCT Somatom Drive (Siemens Healthineers), with the use of standard tube voltage and tube current settings. While in the supine position, patients underwent CT without IV contrast medium but with suspended end-inspiration. After contiguous 8 or 10 mm chest CT sections were obtained, images were reconstructed with a slice thickness of 1.00 mm. All images were photographed at window levels appropriate for the lung parenchyma (width, 1200 HU; level, -600 HU) and mediastinum (width, 360 HU; level, 55 HU).

CT images were re-evaluated sequentially and independently by two radiologists with 10 and 15 years of experience. CT findings were recorded as present or absent on images with a slice thickness of 1.00 mm. The imaging findings that we evaluated included ground-glass opacity, consolidation, involved lung lobes(which?), subpleural line, crazy paving sign, diffuse distribution (involved five lobes), peripheral or bronchovascular distribution, bronchial wall thickening, air bronchogram, halo sign, nodular appearance lymphadenopathy (short-axis diameter >1 cm), and pleural effusion (10,11).

Statistical Analysis

The findings were analyzed by IBM SPSS Statistics for Windows, version 22 (IBM Corp., Armonk, N.Y., USA). CT findings were compared between groups by chi-square rest, and scale variables were compared using the t-test. Finally, significant findings for the H1N1 or COVID-19 groups were evaluated by logistic regression analysis.

RESULTS

A total of 25 patients with H1N1 pneumonia were compared with 150 patients with COVID-19 pneumonia. The median age of COVID-19 pneumonia patients was 54.6±15.9 years, and the median age of H1N1 pneumonia patients was 46.2±12.4 years ($p<0.01$). H1N1 pneumonia patients were younger than COVID-19 pneumonia patients. Findings in all patients are listed in Table 1. The lower lobes were most commonly affected in both lungs. The most frequently observed finding was GGO areas (85.7%). The least frequently observed finding was pleural effusion (10.9%). Of all patients, 110 (62.9%) were male and 65 (37.1%) were female. The distribution between gender and pulmonary findings is shown in Table 2. There was no association between gender and the distribution of pulmonary findings ($p>0.05$). Comparisons of the CT characteristics of H1N1 pneumonia and COVID-19 pneumonia are shown in Table 3. GGO (Figure 1) and consolidation (Figure 2) were present in both H1N1 pneumonia and COVID-19 pneumonia, and no significant difference was observed ($p=0.794$ and $p=0.119$, respectively). The most common site of involvement in COVID-19 and H1N1 pneumonia is the lower lobe of the lung. Based on the distribution pattern, diffuse pattern, peripheral pattern, and bronchopulmonary infiltration were observed more frequently in COVID-19 pneumonia (46.0%, 80.7%, 49.3%, respectively, $p<0.05$). Mediastinal lymphadenopathy and pleural effusion (Figure 3) were observed more frequently in patients with H1N1 pneumonia (24% and 36%, respectively, $p<0.05$). Nodular involvement, crazy paving sign (Figure 4), GGO,

Table 1. Overall summary of the findings

		n	%
Gender	Male	110	62.9%
	Female	65	37.1%
Right upper lobe		111	63.4%
Right middle lobe		112	64.0%
Right lower lobe		146	83.4%
Left upper lobe		112	64.0%
Left lower lobe		151	86.3%
Ground-glass opacities		150	85.7%
Consolidation		115	65.7%
Diffuse pattern		71	40.6%
Peripheral pattern		136	77.7%
Bronchovascular distribution		81	46.3%
Crazy paving sign		54	30.9%
Nodular consolidation		50	28.6%
Air bronchogram		58	33.1%
Halo sign		37	21.1%
Bronchial thickening		25	14.3%
Pleural effusion		19	10.9%
Mediatinal lymphadenopathy		22	12.6%
Subpleural line		56	32.0%
Study groups	COVID-19	150	85.7%
	H1N1	25	14.3%

COVID-19: Coronavirus disease-2019.

consolidation, subpleural line, bronchial wall thickening, halo sign, and air bronchogram did not differ between patients with H1N1 pneumonia and patients with COVID-19 pneumonia (p>0.05). According to logistic regression analysis, advanced age and the presence of a diffuse-peripheral pattern indicated COVID-19. The rate of pleural effusions and mediastinal lymphadenopathy is higher with H1N1 involvement. The distinguishing characteristics for COVID-19 and H1N1 pneumonia according to multivariate analysis are shown in Table 4.

DISCUSSION

The first cases of COVID-19 pneumonia occurred in December 2019 in Wuhan, China. This virus is transmitted from person to person and has caused a pandemic. Because viral pneumonia can be caused by SARS-CoV-2 and H1N1 virus infections, we sought to determine whether there were differences in pneumonia caused by these viruses. The results of the present study showed that mediastinal lymphadenopathy and pleural effusion were more common in patients with H1N1 pneumonia, whereas peripheral and diffuse patterns (involving five lobes) were more common in patients with COVID-19 pneumonia. There were no significant differences in other CT findings. Among the findings of this study, we show that the mean age of COVID-19 pneumonia patients is younger than that of H1N1 pneumonia patients. This finding is consistent with previous studies (11-14).

In our study, peripherally located GGO was observed in 80.7% of patients with COVID-19 pneumonia. Similarly, Song et al. (15) reported a rate of 86% and Xu et al. (16) reported peripheral GGO with a rate of 96.4% in the literature.

Table 2. Distribution of findings according to gender

		Gender				p
		Male		Female		
		n	%	n	%	
Ground-glass opacities	No	13	11.8%	12	18.5%	0.225
	Yes	97	88.2%	53	81.5%	
Consolidation	No	38	34.5%	22	33.8%	0.925
	Yes	72	65.5%	43	66.2%	
Right upper lobe	No involvement	43	39.1%	21	32.3%	0.368
	Involvement	67	60.9%	44	67.7%	
Right middle lobe	No involvement	40	36.4%	23	35.4%	0.896
	Involvement	70	63.6%	42	64.6%	
Right lower lobe	No involvement	19	17.3%	10	15.4%	0.745
	Involvement	91	82.7%	55	84.6%	
Left upper lobe	No involvement	42	38.2%	21	32.3%	0.434
	Involvement	68	61.8%	44	67.7%	
Left lower lobe	No involvement	18	16.4%	6	9.2%	0.185
	Involvement	92	83.6%	59	90.8%	
Diffuse pattern	No	66	60.0%	38	58.5%	0.841
	Yes	44	40.0%	27	41.5%	

Table 2. Continued

		Gender				p
		Male		Female		
		n	%	n	%	
Peripheral pattern	No	27	24.5%	12	18.5%	0.350
	Yes	83	75.5%	53	81.5%	
Bronchovascular distribution	No	60	54.5%	34	52.3%	0.774
	Yes	50	45.5%	31	47.7%	
Crazy paving sign	No	72	65.5%	49	75.4%	0.169
	Yes	38	34.5%	16	24.6%	
Nodular consolidation	No	79	71.8%	46	70.8%	0.882
	Yes	31	28.2%	19	29.2%	
Air bronchogram	No	76	69.1%	41	63.1%	0.414
	Yes	34	30.9%	24	36.9%	
Halo sign	No	87	79.1%	51	78.5%	0.992
	Yes	23	20.9%	14	21.5%	
Bronchial thickening	No	91	82.7%	59	90.8%	0.142
	Yes	19	17.3%	6	9.2%	
Pleural effusion	No	99	90.0%	57	87.7%	0.635
	Yes	11	10.0%	8	12.3%	
Mediatinal lymphadenopathy	No	96	87.3%	57	87.7%	0.936
	Yes	14	12.7%	8	12.3%	
Subpleural line	No	71	64.5%	48	73.8%	0.203
	Yes	39	35.5%	17	26.2%	
Study groups	COVID-19	93	84.5%	57	87.7%	0.565
	H1N1	17	15.5%	8	12.3%	

COVID-19: Coronavirus disease-2019.

Table 3. Distribution of findings according to study groups

		Study groups				p
		COVID-19		H1N1		
		n	%	n	%	
Gender	Male	93	62.0%	17	68.0%	0.565
	Female	57	38.0%	8	32.0%	
Ground-glass opacities	No	21	14.0%	4	16.0%	0.794
	Yes	129	86.0%	21	84.0%	
Consolidation	No	48	32.0%	12	48.0%	0.119
	Yes	102	68.0%	13	52.0%	
Right upper lobe	No involvement	57	38.0%	7	28.0%	0.336
	Involvement	93	62.0%	18	72.0%	
Right middle lobe	No involvement	54	36.0%	9	36.0%	1.000
	Involvement	96	64.0%	16	64.0%	
Right lower lobe	No involvement	23	15.3%	6	24.0%	0.381
	Involvement	127	84.7%	19	76.0%	
Left upper lobe	No involvement	57	38.0%	6	24.0%	0.177
	Involvement	93	62.0%	19	76.0%	

Table 3. Continued

		Study groups				p
		COVID-19		H1N1		
		n	%	n	%	
Left lower lobe	No involvement	18	12.0%	5	20.0%	0.119
	Involvement	132	88.0%	20	80.0%	
Diffuse pattern (involved five lobes)	No	81	54.0%	23	92.0%	<0.001
	Yes	69	46.0%	2	8.0%	
Peripheral pattern	No	29	19.3%	10	40.0%	0.022
	Yes	121	80.7%	15	60.0%	
Bronchovascular distribution	No	76	50.7%	18	72.0%	0.048
	Yes	74	49.3%	7	28.0%	
Crazy paving sign	No	103	68.7%	18	80.0%	0.643
	Yes	47	31.3%	7	20.0%	
Nodular consolidation	No	108	72.0%	20	72.0%	0.738
	Yes	42	28.0%	5	28.0%	
Air bronchogram	No	102	68.0%	15	60.0%	0.431
	Yes	48	32.0%	10	40.0%	
Halo sign	No	118	78.7%	20	80.0%	0.880
	Yes	32	21.3%	5	20.0%	
Bronchial thickening	No	131	87.3%	19	76.0%	0.134
	Yes	19	12.7%	6	24.0%	
Pleural effusion	No	137	91.3%	19	76.0%	0.034
	Yes	13	8.7%	6	24.0%	
Mediatinal lymphadenopathy	No	137	91.3%	16	64.0%	0.001
	Yes	13	8.7%	9	36.0%	
Subpleural line	No	103	68.7%	20	80.0%	0.643
	Yes	47	31.3%	5	20.0%	

COVID-19: Coronavirus disease-2019.

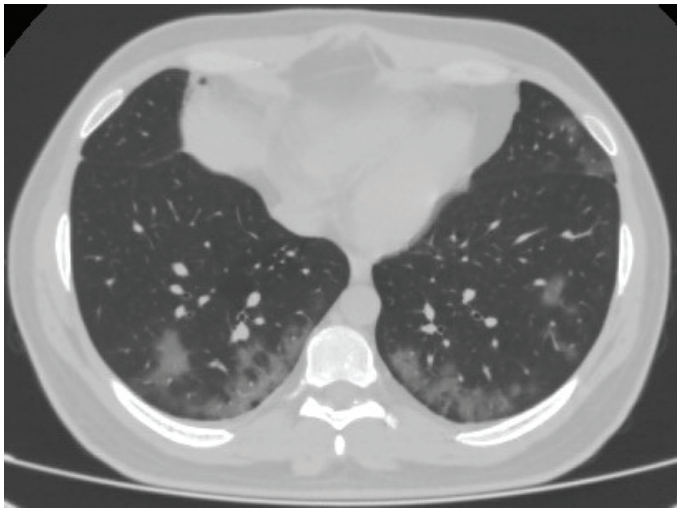

Figure 1. GGO consistent with peripherally located COVID-19 pneumonia is found in both lower lobes of the lungs.

GGO: Ground glass opacities, COVID-19: Coronavirus disease-2019.

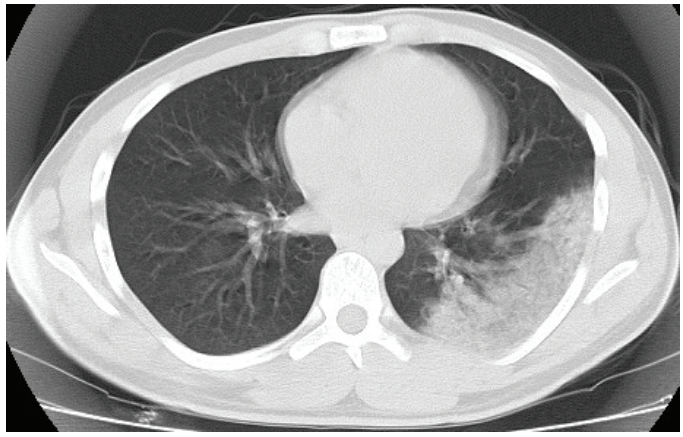

Figure 2. A large peripherally located consolidation area is observed in the lower lobe of the left lung.

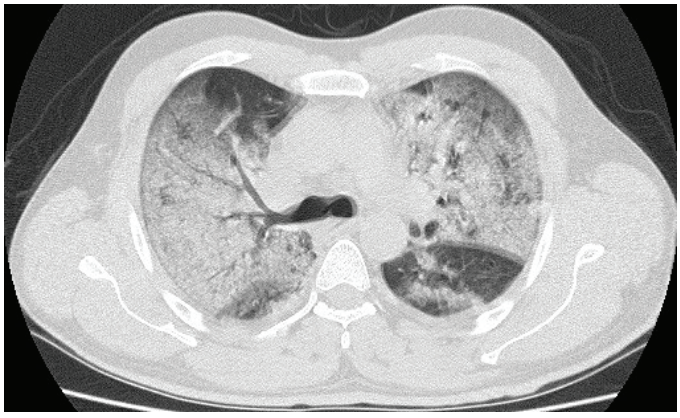

Figure 3. Diffuse GGO consolidation areas consistent with H1N1 pneumonia are observed in the upper lobes of both lungs. Effusion is present in both pleural spaces.

GGO: Ground glass opacities.

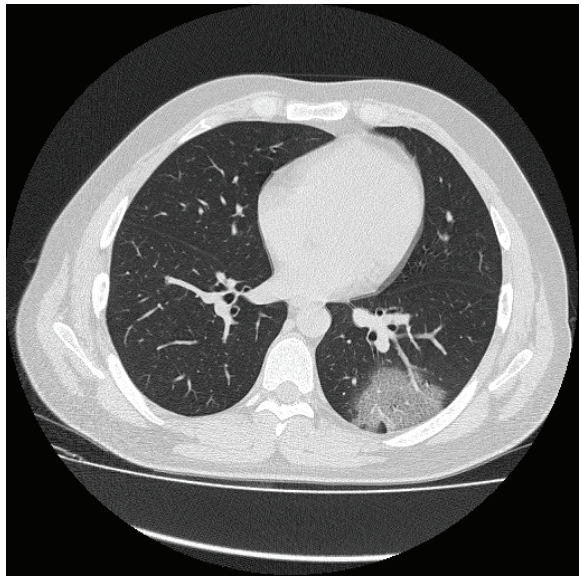

Figure 4. A patient diagnosed with COVID-19 pneumonia in the lower lobe of the left lung with a peripheral localized crazy paving sign.

COVID-19: Coronavirus disease-2019.

Table 4. Distinguishing features of COVID-19 and H1N1 pneumonia according to multivariate analysis. Advanced age and the presence of diffuse and peripheral patterns indicate that COVID-19, pleural effusion, and hilar lymphadenopathy are higher in H1N1 involvement

	B	Sig.	Exp(B)	95% CI for Exp(B)	
				Lower	Upper
Age	-0.041	0.031	0.960	0.925	0.996
Diffuse pattern	-1,764	0.029	0.171	0.035	0.834
Peripheral pattern	-1,260	0.026	0.284	0.094	0.860
Bronchovascular distribution	-0.821	0.147	0.440	0.145	1,336
Pleural effusion	0.949	0.201	2,582	0.603	11,055
Mediastinal lymphadenopathy	2,071	0.002	7,933	2,193	28,702
Constant	0.817	0.461	2,263		

Sig.: Significance, COVID-19: Coronavirus disease-2019, CI: Confidence interval.

In the present study, we found a diffuse distribution pattern (involvement of five lung lobes) more frequently in COVID-19 pneumonia than in H1N1 pneumonia. Kuang et al. (11) and Liu et al. (17) reported that the diffuse distribution pattern was more common in H1N1 pneumonia. Similarly, the diffuse distribution pattern was generally reported in the literature as a more frequent finding for H1N1 pneumonia. The reason why we found the opposite result in our study can be explained by the fact that our hospital is a tertiary hospital and patients with severe COVID-19 pneumonia in our region are followed up in our hospital.

Consolidation and GGO are common in both types of pneumonia. Consolidation has been reported as a second dominant feature in COVID-19 patients within a few days of disease onset. The presence of consolidation may indicate an increase in disease severity (18). In our present study, GGO was observed in 86% and consolidation in 68% of patients with COVID-19 pneumonia, whereas GGO was observed in 84% and consolidation in 52% of patients with H1N1 pneumonia. No difference was found between pneumonia in consolidation and GGO (0.119 and 0.794, respectively). Yin et al. (10) obtained similar results in their study.

Which lobe is more commonly involved and do the involved lobes help in diagnosis? We compared involvement in the five lobes of the lung and found no significant results. However, diffuse patterns and peripheral distribution patterns are more common in COVID-19 pneumonia. In the study by Kuang et al. (11), no association was found between the lobes involved, but peripheral and diffuse distributions were found to be significant in relation to COVID-19 pneumonia. This is in agreement with the results of our current study. Mediastinal lymphadenopathy and pleural effusion are relatively rare findings in COVID-19 pneumonia (19). These findings are also observed in relatively low numbers of H1N1 pneumonia. However, the findings of mediastinal lymphadenopathy and pleural effusion were significantly higher in H1N1 pneumonia than in COVID-19 pneumonia. In a study by Valente et al. (20), 14.3% of patients with H1N1 pneumonia had mediastinal lymphadenopathy ($p<0.001$), and Onigbinde et al. (21) also emphasized this finding in his study.

In some studies reviewed, the incidence of lymphadenopathy was low in patients with COVID-19 pneumonia. In one study, lymphadenopathy was observed in 2.7% of COVID-19 patients and in 10.0% of non-COVID-19 patients (p<0.001) (22). However, the presence of lymphadenopathy is considered an important risk factor for severe COVID-19 pneumonia and is probably due to bacterial superinfection (23). In our study, pleural effusion was a rare finding in COVID-19 pneumonia, and similar findings have been reported in previous studies (21,24). In Yin et al. (10), the frequency of pleural effusion was increased in H1N1 pneumonia compared with COVID-19 pneumonia (p=0.002). Our results were consistent with those reported in the literature.

The results show that mediastinal lymphadenopathy and pleural effusion are more common in patients with H1N1 pneumonia, whereas diffuse peripheral distribution is more common in patients with COVID-19 pneumonia. Other CT features, including nodular appearance, crazy paving sign, GGO, consolidation, subpleural line, bronchial wall thickening, halo sign, and air bronchogram, did not differ between patients with H1N1 pneumonia and those with COVID-19 pneumonia.

Crazy paving sign refers to the presence of ground-glass opacities with superimposed interlobular septal thickening and intralobular septal thickening on chest CT. It is a non-specific finding that can occur in many diseases. Recently, a study found that the crazy paving sign occurs in the third week after the onset of symptoms and indicates an advanced stage of the disease (23). Studies have indicated that it increases in COVID-19 pneumonia (10,11,25). However, no significant difference was found in our study (p=0.643). In the study of Lin et al. (1), patients with H1N1 pneumonia and COVID-19 pneumonia were compared, and no significant difference was found in terms of crazy paving sign (p=1.000). In the proportional analysis of our patients, 31.3% of patients with COVID-19 pneumonia and 20% of patients with H1N1 pneumonia showed a crazy paving sign in favor of COVID-19 pneumonia. We believe that the lack of statistical significance in our study is due to the small number of H1N1 pneumonia patients.

Study Limitations

This study has some limitations. Our study was retrospective. This is because the time periods during which COVID-19 pneumonia and H1N1 pneumonia occurred after the SARS-CoV-2 epidemic were different. The number of H1N1 pneumonia cases included was relatively small. The cases may have represented different stages of the disease, resulting in differences in the appearance of radiological findings. Because this study was retrospective, it may be necessary to consider that individuals with H1N1 pneumonia and COVID-19 pneumonia could have additional infections or coinfections, which could lead to differences in imaging between individuals.

CONCLUSION

We found that most of the lesions caused by COVID-19 pneumonia were located in the peripheral region and near the pleura, whereas the diffuse distribution (five-lobe involvement) was randomly distributed and the lesions caused by influenza virus pneumonia were located far from the pleura. Mediastinal lymphadenopathy and pleural effusion were more prominent in influenza virus pneumonia than in COVID-19 pneumonia. These symptoms should be considered in the differential diagnosis of COVID-19 or H1N1 pneumonia when evaluating patients using chest CT.

Ethics

Ethics Committee Approval: The study protocol was approved by the Mardin Provincial Health Directorate Scientific Study Board (approval number: E-37201737-949).

Informed Consent: Retrospective study.

Authorship Contributions

Surgical and Medical Practices: S.Ş., C.A.Ö., Concept: S.Ş., C.A.Ö., Design: S.Ş., C.A.Ö., Data Collection or Processing: S.Ş., C.A.Ö., Analysis or Interpretation: S.Ş., C.A.Ö., Literature Search: S.Ş., C.A.Ö., Writing: S.Ş., C.A.Ö.

Conflict of Interest: No conflict of interest was declared by the authors.

Financial Disclosure: The authors declared that this study received no financial support.

REFERENCES

1. Lin L, Fu G, Chen S, Tao J, Qian A, Yang Y, et al. CT manifestations of coronavirus disease (COVID-19) pneumonia and influenza virus pneumonia: A comparative study. Am J Roentgenol. 2021; 216: 71-9.
2. Eslambolchi A, Maliglig A, Gupta A, Gholamrezanezhad A. COVID-19 or non-COVID viral pneumonia: How to differentiate based on the radiologic findings? World J Radiol. 2020; 12: 289-301.
3. Ai T, Yang Z, Hou H, Zhan C, Chen C, Lv W, et al. Correlation of Chest CT and RT-PCR Testing for Coronavirus Disease 2019 (COVID-19) in China: A Report of 1014 Cases. Radiology. 2020; 296: 32-40.
4. Fu F, Lou J, Xi D, Bai Y, Ma G, Zhao B, et al. Chest computed tomography findings of coronavirus disease 2019 (COVID-19) pneumonia. Eur Radiol 2020; 30: 5489-98.
5. Pandemic (H1N1) 2009 - update 96 [Internet]. [cited 2022 Aug 4]. Available from: https://www.who.int/emergencies/disease-outbreak-news/item/2010_04_16-en
6. Henzler T, Meyer M, Kalenka A, Alb M, Schmid-Bindert G, Bartling S, et al. Image Findings of Patients with H1N1 Virus Pneumonia and Acute Respiratory Failure. Acad Radiol. 2010; 17: 681-5.
7. Amorim VB, Rodrigues RS, Barreto MM, Zanetti G, Marchiori E. Computed tomography findings in patients with H1N1 influenza A infection. Radiol Bras. 2013; 46: 299-306.
8. Ajlan AM, Quiney B, Nicolaou S, Müller NL. Swine-origin influenza A (H1N1) viral infection: radiographic and CT findings. AJR Am J Roentgenol. 2009; 193: 1494-9.
9. Amorim VB, Rodrigues RS, Barreto MM, Zanetti G, Hochhegger B, Marchiori E. Influenza A (H1N1) pneumonia: HRCT findings. J Bras Pneumol. 2013; 39: 323-9.
10. Yin Z, Kang Z, Yang D, Ding S, Luo H, Xiao E. A Comparison of Clinical and Chest CT Findings in Patients with Influenza A (H1N1) Virus Infection and Coronavirus Disease (COVID-19). AJR Am J Roentgenol. 2020; 215: 1065-71.
11. Kuang PD, Wang C, Zheng HP, Ji WB, Gao YT, Cheng JM, et al. Comparison of the clinical and CT features between COVID-19 and H1N1 influenza pneumonia patients in Zhejiang, China. Eur Rev Med Pharmacol Sci. 2021; 25: 1135-45.
12. Han R, Huang L, Jiang H, Dong J, Peng H, Zhang D. Early Clinical and CT Manifestations of Coronavirus Disease 2019 (COVID-19) Pneumonia. AJR Am J Roentgenol. 2020; 215: 338-43.

13. Zhao W, Zhong Z, Xie X, Yu Q, Liu J. Relation between Chest CT Findings and Clinical Conditions of Coronavirus Disease (COVID-19) Pneumonia: A Multicenter Study. AJR Am J Roentgenol. 2020; 214: 1072-7.
14. Huang C, Wang Y, Li X, Ren L, Zhao J, Hu Y, et al. Clinical features of patients infected with 2019 novel coronavirus in Wuhan, China. Lancet. 2020; 395: 497-506.
15. Song F, Shi N, Shan F, Zhang Z, Shen J, Lu H, et al. Emerging 2019 Novel Coronavirus (2019-nCoV) Pneumonia. Radiology. 2020; 295: 210-7.
16. Xu YH, Dong JH, An WM, Lv XY, Yin XP, Zhang JZ, et al. Clinical and computed tomographic imaging features of novel coronavirus pneumonia caused by SARS-CoV-2. J Infect. 2020; 80: 394-400.
17. Liu M, Zeng W, Wen Y, Zheng Y, Lv F, Xiao K. COVID-19 pneumonia: CT findings of 122 patients and differentiation from influenza pneumonia. Eur Radiol. 2020; 30: 5463-9.
18. Ye Z, Zhang Y, Wang Y, Huang Z, Song B. Chest CT manifestations of new coronavirus disease 2019 (COVID-19): a pictorial review. Eur Radiol. 2020; 30: 4381-89.
19. Zheng Y, Wang L, Ben S. Meta-analysis of chest CT features of patients with COVID-19 pneumonia. J Med Virol. 2021; 93: 241-9.
20. Valente T, Lassandro F, Marino M, Squillante F, Aliperta M, Muto R. H1N1 pneumonia: our experience in 50 patients with a severe clinical course of novel swine-origin influenza A (H1N1) virus (S-OIV). Radiol Med. 2012; 117: 165-84.
21. Onigbinde SO, Ojo AS, Fleary L, Hage R. Chest Computed Tomography Findings in COVID-19 and Influenza: A Narrative Review. Biomed Res Int. 2020; 2020: 6928368.
22. Bai HX, Hsieh B, Xiong Z, Halsey K, Choi JW, Tran TML, et al. Performance of Radiologists in Differentiating COVID-19 from Non-COVID-19 Viral Pneumonia at Chest CT. Radiology. 2020; 296: 46-54.
23. Shi H, Han X, Jiang N, Cao Y, Alwalid O, Gu J, et al. Radiological findings from 81 patients with COVID-19 pneumonia in Wuhan, China: a descriptive study. Lancet Infect Dis. 2020; 20: 425-34.
24. Marchiori E, Zanetti G, Fontes CA, Santos ML, Valiante PM, Mano CM, et al. Influenza A (H1N1) virus-associated pneumonia: High-resolution computed tomography-pathologic correlation. Eur J Radiol. 2011; 80: 500-4.
25. Li Y, Xia L. Coronavirus Disease 2019 (COVID-19): Role of Chest CT in Diagnosis and Management. AJR Am J Roentgenol. 2020; 214: 1280-6.